

Electron-electron interactions in decoupled graphene layers

Rosario E.V. Profumo,¹ Marco Polini,^{2,*} Reza Asgari,³ Rosario Fazio,⁴ and A.H. MacDonald⁵

¹*NEST, Istituto Nanoscienze-CNR and Dipartimento di Fisica dell'Università di Pisa, I-56127 Pisa, Italy*

²*NEST, Istituto Nanoscienze-CNR and Scuola Normale Superiore, I-56126 Pisa, Italy*

³*School of Physics, Institute for Research in Fundamental Sciences (IPM), Tehran 19395-5531, Iran*

⁴*NEST, Scuola Normale Superiore and Istituto Nanoscienze-CNR, I-56126 Pisa, Italy*

⁵*Department of Physics, The University of Texas at Austin, Austin, Texas 78712, USA*

Multi-layer graphene on the carbon face of silicon carbide is an intriguing electronic system which typically consists of a stack of ten or more layers. Rotational stacking faults in this system dramatically reduce inter-layer coherence. In this article we report on the influence of inter-layer interactions, which remain strong even when coherence is negligible, on the Fermi liquid properties of charged graphene layers. We find that inter-layer interactions increase the magnitudes of correlation energies and decrease quasiparticle velocities, even when remote-layer carrier densities are small, and that they lessen the influence of exchange and correlation on the distribution of carriers across layers.

PACS numbers: 73.21.Ac,81.05.ue,73.22.Pr,71.10.-w

I. INTRODUCTION

Graphene layers prepared by the thermal decomposition of silicon carbide (SiC)^{1–9} might play a pivotal role in carbon-based analog electronics because of their high carrier mobilities, and because of the possibility of direct growth on a well understood single-crystal semiconductor substrate. This form of graphene, usually termed *epitaxial graphene*, can be grown directly on either silicon or carbon terminated faces of SiC and is scalable to large area circuits.

Epitaxial graphene on the carbon face typically consists of tens of graphene layers (see however Ref. 10), with rotational stacking faults that lead to an electronic structure which is practically indistinguishable^{11–18} from that of a sample with many electrically isolated single-layer graphene (SLG)¹⁹ layers. It is commonly believed^{1–9,11,13,16} that the layer closest to the SiC typically has a rather high carrier density $\approx 10^{12} \text{ cm}^{-2}$, due to charge transfer from the substrate, and that the overlayers are nearly neutral and unimportant for most observables. Even though multi-layer graphene (MLG) on the C-face of SiC has been shown to possess many of the distinctive features of SLG, including the half-quantized quantum Hall effect^{10,20}, two key questions arise: i) to what extent do Coulomb interactions between electrons in nearby layers distinguish the electronic properties of MLG layers from those of SLG? ii) what is the role of inter-layer Coulomb interactions in determining the electron-density distribution which achieves equilibrium between layers? These are the main issues we address in this article.

The system we study is sketched in Fig. 1. We assume that the graphene layers are perfectly decoupled from the point of view of single-particle tunneling, but take Coulomb interactions between electrons in different layers, which provide a source of (two-particle) coupling, fully into account. We study, (i) the impact of intra- and inter-layer Coulomb interactions on the Fermi-liquid properties of MLG two-dimensional electron sys-

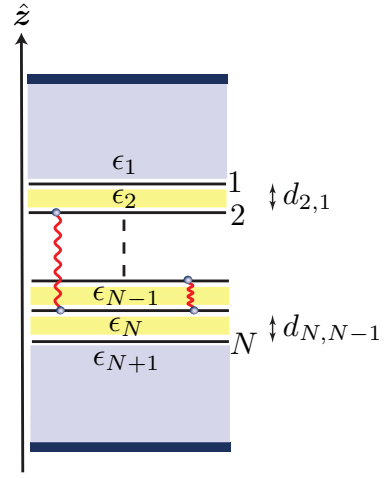


FIG. 1: (Color online) A stack of $\ell = 1 \dots N$ graphene layers is placed between top and bottom dielectrics. The layers are coupled solely by inter-layer Coulomb interactions (red wiggly lines). The dielectric constant in the region above the ℓ -th layer is labeled by ϵ_ℓ , while the one of the substrate is labeled by ϵ_{N+1} . The separation between the $\ell+1$ -th and the ℓ -th layer is labeled by $d_{\ell+1,\ell}$.

tems, and (ii) the combined role of Hartree, exchange, and correlation potentials in determining the equilibrium distribution of carrier densities across layers when charge is transferred to the many-layer system from the SiC substrate. The theory sketched below applies to MLG on the C-face of SiC with an arbitrary number N of layers, to the decoupled layers sometimes found on the surface of bulk graphite²¹, and to the experiments by Schmidt *et al.*²² on micromechanically exfoliated decoupled layers. For the sake of definiteness and simplicity, we present explicit numerical results only for n -type carriers and for the $N = 2$ (double-layer) case.

This manuscript is organized as follows. In Sect. II we present the model we have used to describe tunnel-decoupled graphene layers in the presence of intra- and

inter-layer electron-electron interactions, and discuss the linear-response functions which control the physical properties in which we are interested. In Sect. III we describe the minimal microscopic theory that allows us to calculate quasiparticle velocities, ground-state energies, and chemical potentials. In Sect. IV we present a general scheme to tackle the electro-chemical equilibrium problem in MLG. Finally, in Sect. V we present our main numerical results for double-layer graphene. Sect. VI contains a summary of our main conclusions. Appendix A collects some lengthy expressions for the exchange and correlation energies of double-layer graphene that are important for the technical details of our calculations.

II. MODEL HAMILTONIAN AND LINEAR-RESPONSE THEORY

Our model Hamiltonian contains massless-Dirac-fermion kinetic-energy terms and intra- and inter-layer Coulomb interactions:

$$\hat{\mathcal{H}} = \hbar v \sum_{\mathbf{k}, \ell, \alpha, \beta} \hat{\psi}_{\mathbf{k}, \ell, \alpha}^\dagger (\boldsymbol{\sigma}_{\alpha\beta} \cdot \mathbf{k}) \hat{\psi}_{\mathbf{k}, \ell, \beta} + \frac{1}{2S} \sum_{\mathbf{q} \neq 0, \ell, \ell'} V_{\ell\ell'}(\mathbf{q}) \hat{\rho}_{\mathbf{q}, \ell} \hat{\rho}_{-\mathbf{q}, \ell'} . \quad (1)$$

Here v is the bare Fermi velocity, taken to be the same in all the $\ell = 1 \dots N$ tunnel-decoupled layers, S is the area of each layer, $V_{\ell\ell'}(\mathbf{q})$ is the matrix of bare Coulomb potentials, and

$$\hat{\rho}_{\mathbf{q}, \ell} = \sum_{\mathbf{k}, \alpha} \hat{\psi}_{\mathbf{k}-\mathbf{q}, \ell, \alpha}^\dagger \hat{\psi}_{\mathbf{k}, \ell, \alpha} \quad (2)$$

is the density-operator for the ℓ -th layer. Greek letters are honeycomb-sublattice-pseudospin labels and $\boldsymbol{\sigma} = (\sigma^x, \sigma^y)$ is a vector of Pauli matrices. We also introduce the coupling constant¹⁹ $\alpha_{ee} = e^2/(\hbar v)$, whose value is ≈ 2.2 if for v we use the SLG Fermi velocity $v_F \approx 10^6$ m/s.

Several important many-body properties of the Hamiltonian $\hat{\mathcal{H}}$ are completely determined by the $N \times N$ symmetric matrix $\boldsymbol{\chi}(q, \omega)$ whose elements are the density-density linear-response functions

$$\chi_{\ell\ell'}(q, \omega) = \frac{1}{S} \langle \langle \hat{\rho}_{\mathbf{q}, \ell}; \hat{\rho}_{-\mathbf{q}, \ell'} \rangle \rangle_\omega , \quad (3)$$

with $\langle \langle \hat{A}, \hat{B} \rangle \rangle_\omega$ the usual Kubo product²³. Within the random phase approximation (RPA) these functions satisfy the following matrix equation,

$$\boldsymbol{\chi}^{-1}(q, \omega) = \boldsymbol{\chi}_0^{-1}(q, \omega) - \mathbf{V}(q) , \quad (4)$$

where $\boldsymbol{\chi}_0(q, \omega)$ is a $N \times N$ diagonal matrix whose elements $\chi_\ell^{(0)}(q, \omega)$ are the well-known²⁴⁻²⁶ noninteracting (Lindhard) response functions of each graphene layer at arbitrary doping $n_\ell = N_\ell/S$. The off-diagonal (diagonal) elements of the matrix $\mathbf{V} = \{V_{\ell\ell'}\}_{\ell, \ell'=1 \dots N}$ represent inter-layer (intra-layer) Coulomb interactions.

III. QUASIPARTICLE VELOCITIES, GROUND-STATE ENERGY, AND CHEMICAL POTENTIALS

The Fermi-liquid parameters of MLG can be calculated from the knowledge of the retarded quasiparticle self-energy Σ_ℓ . Our results are based on the so-called ‘‘G₀W’’ approximation^{23,27-30} in which the self-energy Σ_ℓ is expanded to first order in the dynamically screened effective interaction \mathbf{W} ²³,

$$\mathbf{W}(q, \omega) = \mathbf{V}(q) + \mathbf{V}(q) \boldsymbol{\chi}(q, \omega) \mathbf{V}(q) = [\mathbf{V}^{-1}(q) - \boldsymbol{\chi}_0(q, \omega)]^{-1} . \quad (5)$$

In this paper we limit our attention to many-body quantities that can be expressed solely in terms of integrals along the imaginary frequency axis where the Lindhard function has a smooth dependence on its parameters.

The microscopic expression for Σ_ℓ in terms of \mathbf{W} can be obtained by a straightforward generalization of the theory of Ref. 29 to a multicomponent system ($\hbar = 1$):

$$\Sigma_\ell(\mathbf{k}, i\omega_n) = -\frac{1}{\beta} \sum_s \int \frac{d^2\mathbf{q}}{(2\pi)^2} \sum_{m=-\infty}^{+\infty} W_{\ell\ell}(q, i\Omega_m) \times \left[\frac{1 + s \cos(\theta_{\mathbf{k}, \mathbf{k}'})}{2} \right] G_{\ell, s}^{(0)}(\mathbf{k}', i\omega'_{n, m}) , \quad (6)$$

where $\beta = (k_B T)^{-1}$, $\mathbf{k}' = \mathbf{k} + \mathbf{q}$ and $\omega'_{n, m} = \omega_n + \Omega_m$. In Eq. (6) $\omega_n = (2n + 1)\pi/\beta$ is a fermionic Matsubara frequency while the sum runs over all the bosonic Matsubara frequencies $\Omega_m = 2m\pi/\beta$. The factor in square brackets in Eq. (6), which depends on the angle $\theta_{\mathbf{k}, \mathbf{k}+\mathbf{q}}$ between \mathbf{k} and $\mathbf{k} + \mathbf{q}$, captures the dependence of Coulomb scattering on the relative chirality s of the interacting electrons. The Green’s function $G_{\ell, s}^{(0)}(\mathbf{k}, i\omega) = 1/[i\omega - \xi_{\ell, s}(\mathbf{k})]$ describes the free propagation of states with wavevector \mathbf{k} , Dirac energy $\xi_{\ell, s}(\mathbf{k}) = svk - \mu_\ell$ (relative to the chemical potential μ_ℓ of the ℓ -th layer) and chirality $s = \pm$. Note that in the r.h.s. of Eq. (6) there are no terms involving products of the form $W_{\ell\ell'} G_{\ell', s}^{(0)}$ with $\ell' \neq \ell$. The reason is that, due to the absence of inter-layer tunneling, bare propagators are diagonal in the layer index: in the diagrammatic language (see Fig. 8.17 in Ref. 23), screened interaction $W_{\ell\ell'}$ wavy lines closed on a bare propagator cannot begin on layer label ℓ and terminate on layer label $\ell' \neq \ell$.

After analytic continuation from imaginary to real frequencies, $i\omega \rightarrow \omega + i\eta$, the renormalized Fermi velocity v_ℓ^* for the quasiparticles in the ℓ -th layer can be expressed in terms of the wavevector and frequency derivatives of the retarded self-energy $\Sigma_\ell^{\text{ret}}(\mathbf{k}, \omega)$ evaluated at the Fermi surface ($k = k_{F, \ell}$) and at the quasiparticle pole $\omega = \xi_{\ell, +}(\mathbf{k})$:

$$\frac{v_\ell^*}{v} = \frac{1 + (v)^{-1} \partial_k \Re e \Sigma_\ell^{\text{ret}}(\mathbf{k}, \omega) \big|_{k=k_{F, \ell}; \omega=0}}{1 - \partial_\omega \Re e \Sigma_\ell^{\text{ret}}(\mathbf{k}, \omega) \big|_{k=k_{F, \ell}; \omega=0}} . \quad (7)$$

As explained elsewhere^{23,28,29}, the derivatives in Eq. (7)

can both be expressed in terms of integrals along the imaginary frequency axis.

The ground-state energy of MLG can be easily evaluated from $\hat{\mathcal{H}}$. Apart from the trivial kinetic energy contribution $\delta\varepsilon_{\text{kin}}$ related to the first term in $\hat{\mathcal{H}}$, it contains intra- and inter-layer interaction energy contributions. To evaluate the interaction energy we have followed a familiar strategy^{23,24} by combining the coupling-constant integration algorithm with the fluctuation-dissipation theorem^{23,24}. Following Ref. 24, we choose the total energy of undoped MLG (Fermi energy at the neutrality point in all layers) as our zero of energy. We separate the contribution that is first order in α_{ee} , the exchange energy, from the higher order contributions conventionally referred to in electron-gas theory as the correlation energy. Generalizing the theory for SLG²⁴ to a multi-component system, we end up with rather cumbersome expressions for the exchange $\delta\varepsilon_{\text{x}}$ and RPA correlation energies $\delta\varepsilon_{\text{c}}^{\text{RPA}}$ of MLG (per electron) measured from the reference undoped system. Explicit expressions for the $N = 2$ case have been reported in Appendix A. Because these expressions involve only imaginary axis frequency integrals they are easy to evaluate accurately by quadrature.

The determination of the electro-chemical equilibrium, discussed in more detail below, requires knowledge of exchange and correlations contributions to the chemical potentials μ_{ℓ} . These can be easily calculated from

$$\mu_{\ell} = \frac{\partial(n\delta\varepsilon_{\text{tot}})}{\partial n_{\ell}}, \quad (8)$$

where $n = n_1 + n_2 + \dots + n_N$ is the total density and $\delta\varepsilon_{\text{tot}} = \delta\varepsilon_{\text{kin}} + \delta\varepsilon_{\text{x}} + \delta\varepsilon_{\text{c}}^{\text{RPA}}$ is the total energy per electron, a function of n_1, \dots, n_N .

IV. ELECTRO-CHEMICAL EQUILIBRIUM

The equilibrium density distribution across a multi-layer is achieved when the electro-chemical potentials in each distinct electronic region are identical. For a N -layer graphene system grown on a (SiC, say) substrate we identify $N + 1$ electronic regions; the additional system is a buffer layer (not shown in Fig. 1) between the bulk substrate and the graphene layers which is positively charged as a consequence of charge transfer to the graphene system. The equilibrium densities in all the $N + 1$ layers are determined by $N + 1$ equations which express the discontinuity of the electric displacement across charged layers. With the notation introduced in Fig. 1, Gauss's law implies that for $\ell = N, N - 1, \dots, 1$ (from bottom to top)

$$\epsilon_{\ell+1}E_{\ell+1} - \epsilon_{\ell}E_{\ell} = -4\pi e\sigma_{\ell}, \quad (9)$$

where σ_{ℓ} is the areal electron density in the ℓ -th layer. We can view E_1 as a quantity which is determined by a gate voltage. As long as the distance d_{TB} from the top gate

electrode to the MLG system is large, "chemical" potential contributions are negligible so that $eE_1d_{\text{TB}} = V_{\text{TB}}$. We can write down an equation similar to (9) for the buffer layer, $\epsilon_{N+2}E_{N+2} - \epsilon_{N+1}E_{N+1} = +4\pi e\sigma_{\text{b}}$. Again we can view E_{N+2} as an experimentally controllable parameter (fixed by a bottom gate, $eE_{N+2}d_{\text{BG}} = V_{\text{BG}}$). Here σ_{b} is the density of *positive* charges in the buffer layer. This model assumes that the substrate is essentially insulating. In the absence of gates or unintended dopants that might create electric fields, we would normally expect $E_1 = E_{N+2} = 0$. In this case we obtain the charge neutrality condition: $\sum_{\ell=1}^N \sigma_{\ell} = \sigma_{\text{b}}$. In general σ_{b} should not be considered a free parameter. It is determined by the total graphene charge and the difference between the two experimentally fixed electric fields E_1 and E_{N+2} . For MLG samples grown on SiC σ_{b} depends on growth parameters in a way which is at present not well understood.

As explained above, our convention for the zero-of-energy of *chemical* energy of each layer is that it is zero at the Dirac point, *i.e.*, at electrical neutrality. It is convenient to also choose an explicit global zero for the electric potential, which we take to be its value on the top layer. Given the charge densities, the electrical potentials in each layer can be conveniently calculated iteratively starting from the top layer. For $\ell = 1, 2, \dots, N - 1$ we have that

$$V_{\ell+1} = V_{\ell} + eE_{\ell+1}d_{\ell+1,\ell}. \quad (10)$$

Here $d_{\ell+1,\ell}$ is the separation between the $\ell + 1$ -th and the ℓ -th layer. The condition for equilibrium between a graphene layer and the layer below it is:

$$\mu_{\ell+1} + V_{\ell+1} = \mu_{\ell} + V_{\ell}. \quad (11)$$

We need one more equation to fix the densities and that is the equilibrium condition between the bottom layer and the buffer: $V_{\text{b}} + \phi = V_N + \mu_N$. Here ϕ represents the microscopic physics which causes electrons to spill out of the buffer layer (where they are likely poorly bonded). It is known that ϕ is sensitive to the arrangement of carbon atoms in the buffer layer. If all of the graphene layers are negatively charged there will be a large electric field between the N -th layer and the buffer layer whose sign will tend to repel electrons, *i.e.* to make $V_{\text{b}} < V_N$. The value of ϕ must therefore be positive and it should be chosen to match experimental results for the total charge of all layers in a MLG systems. We assume that ϕ is fixed once a sample has been prepared, *i.e.* that it is not influenced by gate voltages, external magnetic fields, or other parameters that are routinely used to alter the electrical properties of two dimensional electron systems.

V. NUMERICAL RESULTS AND DISCUSSION

We now turn to the presentation of detailed illustrative numerical results for double-layer graphene (DLG).

The bare intra- and inter-layer Coulomb interactions are influenced by the layered dielectric environment. For the $N = 2$ case, a routine electrostatics calculation³¹ implies that the Coulomb interaction in the $\ell = 1$ (top) layer is given by

$$V_{11}(q) = \frac{4\pi e^2}{qD(q)} [(\epsilon_2 + \epsilon_3)e^{qd} + (\epsilon_2 - \epsilon_3)e^{-qd}], \quad (12)$$

where

$$D(q) = [(\epsilon_1 + \epsilon_2)(\epsilon_2 + \epsilon_3)e^{qd} + (\epsilon_1 - \epsilon_2)(\epsilon_2 - \epsilon_3)e^{-qd}] \quad (13)$$

and d is a shorthand notation for the inter-layer distance $d_{2,1}$. The Coulomb interaction in the bottom layer, $V_{22}(q)$, can be simply obtained from $V_{11}(q)$ by interchanging $\epsilon_3 \leftrightarrow \epsilon_1$. Finally, the inter-layer Coulomb interaction is given by

$$V_{12}(q) = V_{21}(q) = \frac{8\pi e^2}{qD(q)} \epsilon_2. \quad (14)$$

In the case $N = 2$ the matrix equation (4) can be easily inverted and the screened potentials \mathbf{W} in Eq. (5) can be written in a particularly compact form³²:

$$W_{11}(q, \omega) = \frac{V_{11}(q) + [V_{12}^2(q) - V_{11}(q)V_{22}(q)]\chi_2^{(0)}(q, \omega)}{\varepsilon(q, \omega)} \quad (15)$$

and

$$W_{12}(q) = \frac{V_{12}(q)}{\varepsilon(q, \omega)}. \quad (16)$$

The expression for $W_{22}(q)$ can be obtained from Eq. (15) by interchanging $1 \leftrightarrow 2$. In Eqs. (15)-(16) we have introduced the dielectric function

$$\begin{aligned} \varepsilon(q, \omega) &= [1 - V_{11}(q)\chi_1^{(0)}(q, \omega)][1 - V_{22}(q)\chi_2^{(0)}(q, \omega)] \\ &\quad - V_{12}^2(q)\chi_1^{(0)}(q, \omega)\chi_2^{(0)}(q, \omega). \end{aligned} \quad (17)$$

Exchange and correlation energies in MLG systems depend both on interactions on the Fermi wavelength scale which influence correlations between carriers and on interactions at shorter length scales which influence correlation with the Dirac sea background. This contrasts sharply with the case of ordinary two-dimensional electron gases for which many-body properties depend only on interactions on the Fermi wavelength scale. Because MLG layers are separated by atomic length scales and carrier densities are always small on atomic scales $k_F \ell d$ is typically small. Taking the limit $qd \rightarrow 0$ in Eqs. (12)-(14) we find that the typical carrier-carrier interactions are layer independent with effective dielectric constant $(\epsilon_1 + \epsilon_3)/2$. Similarly, taking the limit $qd \rightarrow \infty$ we find that carrier-background interactions are approximately independent in different layers, and that they have an effective dielectric constant determined mostly by immediately adjacent layers.

With these explicit expressions in our hands we are in the position to calculate the quasiparticle self-energies Σ_ℓ and velocities v_ℓ^* , the exchange $\delta\varepsilon_x$ and RPA correlation $\delta\varepsilon_c^{\text{RPA}}$ energies, and to solve the electro-chemical equilibrium problem outlined above. For the presentation of the numerical results for the double-layer system we introduce the density polarization $\zeta = (n_2 - n_1)/n$: $\zeta = 1$ when the carrier density is non-zero only in the bottom layer, while $\zeta = 0$ when the two layers have identical carrier densities.

In Fig. 2 we present results for the quasiparticle velocity enhancements in the low and high density layers, v_1^*/v and v_2^*/v , as functions of their carrier density for several different values of the density in the opposite layer. The quasiparticle velocity in a single-layer has a large enhancement due mainly^{29,33} to exchange interactions between the carriers and the Dirac sea. Carrier-carrier interactions yield positive contributions to both the wavevector and frequency dependence of the self-energy, which partially cancel as contributions to the renormalized quasiparticle velocity much as they do in the ordinary two-dimensional electron gas. The end result is that the enhanced velocity due to exchange interactions with the Dirac sea largely survives, especially at low carrier densities. The parameters of this calculation were chosen with DLG on SiC in mind. The general result is that enhanced quasiparticle velocity again survives, with quantitative changes due to electron-electron interactions. Two aspects of these results may appear counter-intuitive at first glance. First of all, we see that inter-layer interactions are important even when the carrier density in remote layers is zero. Because the Dirac bands are gapless and because both bands have π -orbital character, their wavevector and frequency dependent polarization function is important in forming the dynamically screened Coulomb interaction even in the absence of carriers. Secondly, we notice that increasing the density of a remote layer does not necessarily weaken the screened interaction in the layer of interest. The origin of this property can be traced to the second term in Eq. (15) which is not intuitive and captures the mutual screening response of double-layers including inter-layer interaction effects.

In Fig. 3 we present numerical results for the DLG exchange and RPA correlation energies per carrier, $\delta\varepsilon_x$ and $\delta\varepsilon_c^{\text{RPA}}$. In this case we plot energies as a function of total carrier density for several different layer polarizations in order to illustrate a relationship to well known dependences on spin-polarization that we discuss below. Exchange energies are positive because^{24,34} they are calculated relative to zero carrier density using the Dirac point self-energy of this limit as the zero of energy. The increase in exchange energy with carrier density in graphene has the physical consequence that corrections to the RPA are expected³⁴ to enhance screening, instead of weakening it as in an ordinary two-dimensional electron gas. Notice that the exchange energy of DLG is larger than that of SLG. The two are equal for $\zeta = 1$

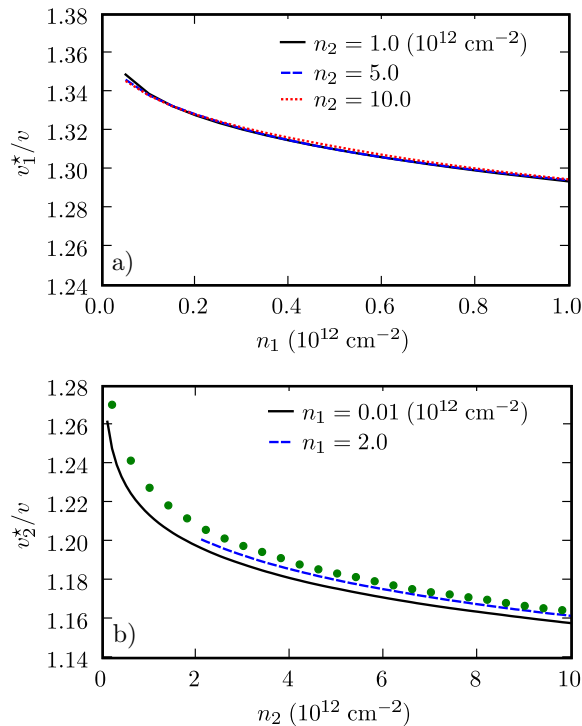


FIG. 2: (Color online) Quasiparticle velocities in double-layer graphene on SiC [$\epsilon_1 = \epsilon_2 = 1.0$ and $\epsilon_3 = 6.6$ (SiC dielectric constant)]. The data shown in this figure have been obtained by setting $d = 3.35$ Å and $\alpha_{ee} = 2.2$. Panel a) Quasiparticle velocity v_1^* in the top layer (in units of the bare velocity v) as a function of the density n_1 in that layer (in units of 10^{12} cm $^{-2}$), for different values of the density n_2 in the opposite layer. Panel b) Quasiparticle velocity v_2^* in the bottom layer (in units of the bare velocity v) as a function of the density n_2 in that layer (in units of 10^{12} cm $^{-2}$), for different values of the density n_1 in the opposite layer. Circles label data for the quasiparticle velocity in single-layer graphene²⁹ on SiC.

because the exchange energy depends only on intra-layer interactions [see Eq. (A1) in Appendix A]. The larger exchange energy in the DLG case, in which carriers are separated between two different layers, has an origin similar to the well known increase in the exchange energy of an electron gas when two different spin states are occupied. The correlation energy, which is negative, is dramatically larger in DLG and strongly influenced by inter-layer interactions. These correlation contributions to the energy suggest that exchange-only approximations overestimate the degree to which screening is enhanced by beyond-RPA corrections. When correlation are included, the interaction energy preference for unequal partitioning of density between layers is also strongly reduced. This result has an origin similar to the well known result that exchange-only theories badly overestimate the tendency of interactions to favor enhanced spin polarization in ordinary electron gases.

Finally, in Fig. 4 we present a typical result for the dependence of the equilibrium densities in top and bot-

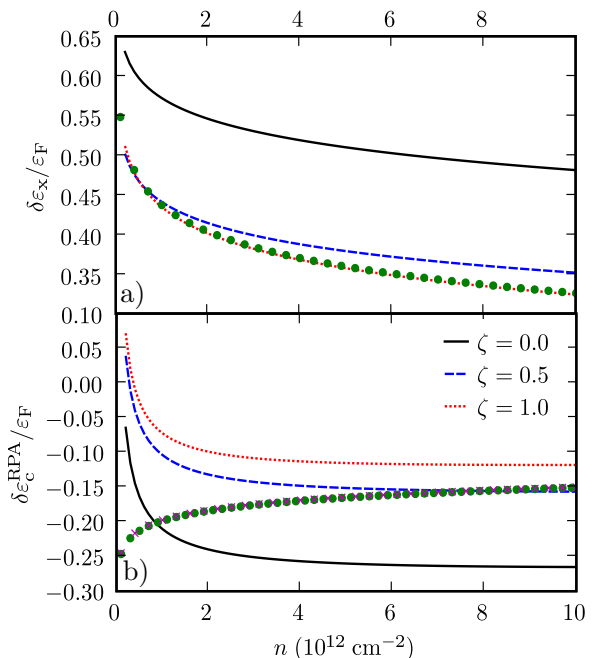


FIG. 3: (Color online) Interaction energies in double-layer graphene on SiC, measured from the reference undoped system. All parameters are the same as in Fig. 2. Panel a) The exchange energy $\delta\epsilon_x$ in units of the Fermi energy ϵ_F as a function of n (in units of 10^{12} cm $^{-2}$) and for different values of ζ . Panel b) Same as in the top panel but for the RPA correlation energy $\delta\epsilon_c^{\text{RPA}}$. Crosses label the RPA correlation energy for $\zeta = 1$ if the inter-layer interaction V_{12} is set to zero. Circles label the exchange and RPA correlation energies in single-layer graphene²⁴ on SiC. Note that the correlation energy obtained neglecting inter-layer interactions (crosses) is practically equal to the single-layer graphene result (circles).

tom layers, n_1^* and n_2^* , on the work function of the buffer layer. We clearly see that the equilibrium density in the top layer n_1^* is substantially smaller than the density in the bottom layer, the ratio n_2^*/n_1^* changing between 1.5 and 3.5 in the range of ϕ values explored in this figure. Quite importantly, note that including e-e interactions at the exchange-only level severely underestimates the values of the equilibrium densities, especially so in the top layer. Including correlation effects reduces the energetic cost of adding electrons to the graphene layers. In fact we find that the increase in exchange energy relative to the Dirac point exchange energy and the decrease in interaction energy due to correlations among the carriers partially compensate, leading to densities in the graphene layers close to those implied by a Hartree theory which completely ignores exchange and correlation effects. This finding is surprising in comparison to the ordinary two-dimensional electron gas case, in which exchange and correlation effects always lower the energy cost of adding carriers and increase charge transferred from an electron reservoir.

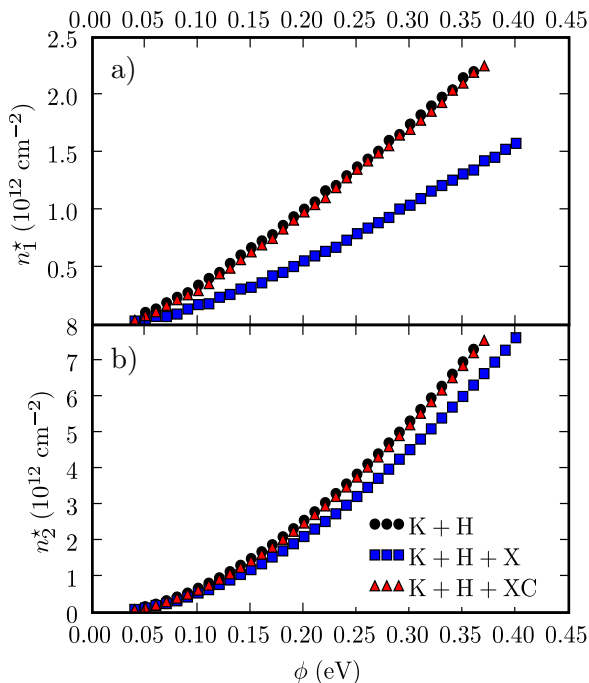


FIG. 4: (Color online) Electro-chemical equilibrium for double-layer graphene on SiC in the absence of top and bottom gates ($E_1 = E_4 = 0$). All parameters are the same as in Figs. 2-3. The distance between buffer and bottom layers is equal to 3.35 Å. Panel a) Equilibrium density in the top layer, n_1^* (in units of 10^{12} cm^{-2}), as a function of the chemical potential ϕ (in eV) in the buffer layer. Here we have reported results obtained (i) neglecting intra- and inter-layer e-e interactions (circles), (ii) including e-e interactions at the exchange-only level (squares), and (iii) including both exchange and correlations (triangles). Panel b) Same as in panel a) but for the bottom layer. Note how $n_2^* > n_1^*$.

VI. SUMMARY AND CONCLUSIONS

In summary, we have presented a theoretical scheme, based on the random phase approximation and on the “ G_0W ” theory, to deal with electron-electron interactions in multi-layer graphene Fermi liquid systems consisting in which hybridization is suppressed by relative rotations of honeycomb lattices. We have presented numerical results for the specific case of a double layer, explicitly demonstrating that inter-layer Coulomb interactions substantially alter the properties of the quasiparticles in this system, with respect to those of isolated single-layer graphene. We have also solved numerically the electro-chemical equilibrium problem, finding that it is crucial to incorporate correlation effects when going beyond a free-electron description of this system. When both effects are included, interactions play a major role in lowering the interaction energy of MLG systems. Because

of strong inter-layer carrier-carrier interactions, the total interaction energy is relatively insensitive to charge distribution among the layers, which is well approximated by a theory that includes only kinetic and electrostatic energies. The unusual positive exchange energy of bilayer graphene acts to suppress charge transfer from the buffer layer. Surprisingly, when both exchange and correlation is included corrections to the Hartree theory of charge transfer from the MLG buffer layer are quite small, at least in the $N = 2$ MLG system. In analysing the physics of larger N MLG systems, it will be essential to recognize that layers contribute to the systems’s exchange and correlation energy even when their carrier density vanishes. Because carrier-carrier interactions are weakly layer dependent, MLG systems might provide an interesting approximate realization of a $SU(N)$ electron gas model in which $1/N$ expansions are quantitatively useful. This might provide an interesting attack on a limit in which corrections to the G_0W theory can be explored by a rigorous semi-classical theory.

Acknowledgments

A.H.M. acknowledges support from the Welch Foundation and from the SWAN NRI program. We thank C. Berger, M. Fogler, and M. Potemski for useful conversations.

Appendix A: Explicit expressions for the exchange and RPA correlation energies of double-layer graphene

For the sake of completeness, in this Appendix we report the expressions we have used to compute the exchange and RPA correlation energies of DLG. In what follows all symbols with a bar over them denote dimensionless quantities. We have scaled all wavevectors with the Fermi wavevector $k_F = \sqrt{\pi n}$ evaluated at the total density n , all frequencies with the Fermi energy $\varepsilon_F = vk_F$, the Lindhard response functions $\chi_\ell^{(0)}$ with the massless Dirac fermion density-of-states $g\varepsilon_F/(2\pi v^2)$, and the bare Coulomb potentials $V_{\ell\ell'}$ with $2\pi e^2/k_F$. Here $g = 4$ is the usual spin-valley degeneracy factor.

It is easy to prove that the exchange energy can be written as

$$\delta\varepsilon_x = - \frac{\varepsilon_F \alpha_{ee}}{\pi} \left\{ \int_0^{+\infty} d\bar{q} \bar{q} \bar{V}_{11}(\bar{q}) \int_0^{+\infty} d\bar{\Omega} \delta\bar{\chi}_1^{(0)}(\bar{q}, i\bar{\Omega}) + \int_0^{+\infty} d\bar{q} \bar{q} \bar{V}_{22}(\bar{q}) \int_0^{+\infty} d\bar{\Omega} \delta\bar{\chi}_2^{(0)}(\bar{q}, i\bar{\Omega}) \right\}, \quad (\text{A1})$$

while the RPA correlation energy as

$$\begin{aligned} \delta\varepsilon_c = & \frac{\varepsilon_F \alpha_{ee}}{\pi} \left\{ \int_0^{+\infty} d\bar{q} \bar{q} \bar{V}_{11}(\bar{q}) \int_0^{+\infty} d\bar{\Omega} \left[\delta\Phi_{11}(\bar{q}, i\bar{\Omega}) + \delta\bar{\chi}_1^{(0)}(\bar{q}, i\bar{\Omega}) \right] \right. \\ & \left. + \int_0^{+\infty} d\bar{q} \bar{q} \bar{V}_{22}(\bar{q}) \int_0^{+\infty} d\bar{\Omega} \left[\delta\Phi_{22}(\bar{q}, i\bar{\Omega}) + \delta\bar{\chi}_2^{(0)}(\bar{q}, i\bar{\Omega}) \right] + 2 \int_0^{+\infty} d\bar{q} \bar{q} \bar{V}_{12}(\bar{q}) \int_0^{+\infty} d\bar{\Omega} \delta\Phi_{12}(\bar{q}, i\bar{\Omega}) \right\}. \end{aligned} \quad (\text{A2})$$

In Eq. (A2) we have introduced the quantities (for reasons of space we will omit to write explicitly the depen-

dence of the following expressions on the variables q and $i\Omega$)

$$\begin{aligned} \Phi_{11} = & -\frac{1}{(g\alpha_{ee})^2 \bar{\chi}_2^{(0)} (\bar{V}_{11} \bar{V}_{22} - \bar{V}_{12}^2)} \left\{ \frac{2L - (g\alpha_{ee}) \bar{V}_{22} \bar{\chi}_2^{(0)} (K + \sqrt{\Delta})}{2\sqrt{\Delta}} \ln \left| \frac{2L - K - \sqrt{\Delta}}{-K - \sqrt{\Delta}} \right| \right. \\ & \left. - \frac{2L - (g\alpha_{ee}) \bar{V}_{22} \bar{\chi}_2^{(0)} (K - \sqrt{\Delta})}{2\sqrt{\Delta}} \ln \left| \frac{2L - K + \sqrt{\Delta}}{-K + \sqrt{\Delta}} \right| \right\} \end{aligned} \quad (\text{A3})$$

and

$$\Phi_{12} = -\frac{\bar{V}_{12}}{(g\alpha_{ee})(\bar{V}_{11}\bar{V}_{22} - \bar{V}_{12}^2)} \left\{ \frac{K + \sqrt{\Delta}}{2\sqrt{\Delta}} \ln \left| \frac{2L - K - \sqrt{\Delta}}{-K - \sqrt{\Delta}} \right| - \frac{K - \sqrt{\Delta}}{2\sqrt{\Delta}} \ln \left| \frac{2L - K + \sqrt{\Delta}}{-K + \sqrt{\Delta}} \right| \right\}, \quad (\text{A4})$$

where

$$\Delta = (g\alpha_{ee})^2 \left[(\bar{V}_{11} \bar{\chi}_1^{(0)} - \bar{V}_{22} \bar{\chi}_2^{(0)})^2 + 4\bar{V}_{12}^2 \bar{\chi}_1^{(0)} \bar{\chi}_2^{(0)} \right], \quad (\text{A5})$$

$$L = (g\alpha_{ee})^2 \left(\bar{V}_{11} \bar{V}_{22} \bar{\chi}_1^{(0)} \bar{\chi}_2^{(0)} - \bar{V}_{12}^2 \bar{\chi}_1^{(0)} \bar{\chi}_2^{(0)} \right), \quad (\text{A6})$$

and

$$K = g\alpha_{ee} \left(\bar{V}_{11} \bar{\chi}_1^{(0)} + \bar{V}_{22} \bar{\chi}_2^{(0)} \right). \quad (\text{A7})$$

The expression for Φ_{22} can be obtained from Eq. (A3) by interchanging $1 \leftrightarrow 2$.

Finally, we remark that all the quantities which in Eqs. (A1)-(A2) are preceded by the sign “ δ ” indicate quantities defined by differences between doped and un-

doped values: for example

$$\delta\bar{\chi}_\ell^{(0)}(\bar{q}, i\bar{\Omega}) = \bar{\chi}_\ell^{(0)}(\bar{q}, i\bar{\Omega}) - \bar{\chi}_\ell^{(0)}(\bar{q}, i\bar{\Omega}) \Big|_{k_F, \ell=0}, \quad (\text{A8})$$

and

$$\delta\Phi_{ij}(\bar{q}, i\bar{\Omega}) = \Phi_{ij}(\bar{q}, i\bar{\Omega}) - \Phi_{ij}(\bar{q}, i\bar{\Omega}) \Big|_{k_F, \ell=0}. \quad (\text{A9})$$

Note that the dimensionless Lindhard function in the undoped limit is the same for every layer and is given by

$$\bar{\chi}_\ell^{(0)}(\bar{q}, i\bar{\Omega}) \Big|_{k_F, \ell=0} = -\frac{\pi}{8} \frac{\bar{q}^2}{\sqrt{\bar{q}^2 + \bar{\Omega}^2}}. \quad (\text{A10})$$

* Electronic address: m.polini@sns.it

- ¹ C. Berger, Z. Song, X. Li, X. Wu, N. Brown, C. Naud, D. Mayou, T. Li, J. Hass, A.N. Marchenkov, E.H. Conrad, P.N. First, and W.A. de Heer, *Science* **312**, 1191 (2006).
- ² E. Rollings, G.-H. Gweon, S.Y. Zhou, B.S. Mun, J.L. McChesney, B.S. Hussain, A.V. Fedorov, P.N. First, W.A. de Heer, and A. Lanzara, *J. Phys. Chem. Solids* **67**, 2172 (2006).
- ³ W.A. de Heer, C. Berger, X. Wu, P.N. First, E.H. Conrad, X. Li, T. Li, M. Sprinkle, J. Hass, Marcin L. Sadowski, M. Potemski, and G. Martinez, *Solid State Commun.* **143**, 92

- (2007).
- ⁴ A. Bostwick, T. Ohta, T. Seyller, K. Horn, and E. Rotenberg, *Nature Phys.* **3**, 36 (2007).
- ⁵ S.Y. Zhou, G.-H. Gweon, A.V. Fedorov, P.N. First, W.A. de Heer, D.-H. Lee, F. Guinea, A.H. Castro Neto, and A. Lanzara, *Nature Mater.* **6**, 770 (2007).
- ⁶ K.V. Emtsev, F. Speck, T. Seyller, L. Ley, and J.D. Riley, *Phys. Rev. B* **77**, 155303 (2008).
- ⁷ K.V. Emtsev, A. Bostwick, K. Horn, J. Jobst, G.L. Kellogg, L. Ley, J.L. McChesney, T. Ohta, S.A. Reshanov, J. Röhrl, E. Rotenberg, A.K. Schmid, D. Waldmann, H.B.

- Weber, and T. Seyller, *Nature Mater.* **8**, 203 (2009).
- ⁸ C. Riedl, C. Coletti, T. Iwasaki, A.A. Zakharov, and U. Starke, *Phys. Rev. Lett.* **103**, 246804 (2009).
- ⁹ P.N. First, W.A. de Heer, T. Seyller, C. Berger, J.A. Stroscio, and J.-S. Moon, arXiv:1002.0873v1.
- ¹⁰ X. Wu, Y. Hu, M. Ruan, N.K. Madiomanana, J. Hankinson, M. Sprinkle, C. Berger, and W.A. de Heer, *Appl. Phys. Lett.* **95**, 223108 (2009).
- ¹¹ M.L. Sadowski, G. Martinez, M. Potemski, C. Berger, and W.A. de Heer, *Phys. Rev. Lett.* **97**, 266405 (2006).
- ¹² X. Wu, X. Li, Z. Song, C. Berger, and W.A. de Heer, *Phys. Rev. Lett.* **98**, 136801 (2007).
- ¹³ F. Varchon, R. Feng, J. Hass, X. Li, B. Ngoc Nguyen, C. Naud, P. Mallet, J.-Y. Veuillen, C. Berger, E.H. Conrad, and L. Magaud, *Phys. Rev. Lett.* **99**, 126805 (2007).
- ¹⁴ J.M. Lopes dos Santos, N.M. Peres, and A.H. Castro Neto, *Phys. Rev. Lett.* **99**, 256802 (2007).
- ¹⁵ J. Hass, F. Varchon, J.E. Millán-Otoya, M. Sprinkle, N. Sharma, W.A. de Heer, C. Berger, P.N. First, L. Magaud, and E.H. Conrad *Phys. Rev. Lett.* **100**, 125504 (2008).
- ¹⁶ M. Orlita, C. Faugeras, P. Plochocka, P. Neugebauer, G. Martinez, D.K. Maude, A.-L. Barra, M. Sprinkle, C. Berger, W.A. de Heer, and M. Potemski, *Phys. Rev. Lett.* **101**, 267601 (2008).
- ¹⁷ F. Varchon, P. Mallet, L. Magaud, and J.-Y. Veuillen, *Phys. Rev. B* **77**, 165415 (2008); F. Hiebel, P. Mallet, F. Varchon, L. Magaud, and J.-Y. Veuillen, *ibid.* **78**, 153412 (2008); L. Magaud, F. Hiebel, F. Varchon, P. Mallet, and J.-Y. Veuillen, *ibid.* **79**, 161405(R) (2009).
- ¹⁸ M. Sprinkle, D. Siegel, Y. Hu, J. Hicks, P. Soukiassian, A. Tejeda, A. Taleb-Ibrahimi, P. Le Fèvre, F. Bertran, C. Berger, W.A. de Heer, A. Lanzara, and E.H. Conrad, *Phys. Rev. Lett.* **103**, 226803 (2009).
- ¹⁹ A.H. Castro Neto, F. Guinea, N.M. Peres, K.S. Novoselov, and A.K. Geim, *Rev. Mod. Phys.* **81**, 109 (2009).
- ²⁰ A. Tzalenchuk, S. Lara-Avila, A. Kalaboukhov, S. Paolillo, M. Syväjärvi, R. Yakimova, O. Kazakova, T.J.B.M. Janssen, V. Fal'ko, and S. Kubatkin, *Nature Nanotech.* **5**, 186 (2010).
- ²¹ G. Li, A. Luican, and E.Y. Andrei, *Phys. Rev. Lett.* **102**, 176804 (2009); P. Neugebauer, M. Orlita, C. Faugeras, A.-L. Barra, and M. Potemski, *ibid.* **103**, 136403 (2009).
- ²² H. Schmidt, T. Luedtke, P. Barthold, and R.J. Haug, *Phys. Rev. B* **81**, 121403(R) (2010).
- ²³ G.F. Giuliani and G. Vignale, *Quantum Theory of the Electron Liquid* (Cambridge University Press, Cambridge, 2005).
- ²⁴ Y. Barlas, T. Pereg-Barnea, M. Polini, R. Asgari, and A.H. MacDonald, *Phys. Rev. Lett.* **98**, 23660 (2007).
- ²⁵ B. Wunsch, T. Stauber, F. Sols, and F. Guinea, *New J. Phys.* **8**, 318 (2006).
- ²⁶ E.H. Hwang and S. Das Sarma, *Phys. Rev. B* **75**, 205418 (2007).
- ²⁷ L. Hedin, *Phys. Rev.* **139**, A796 (1965).
- ²⁸ R. Asgari, B. Davoudi, M. Polini, G.F. Giuliani, M.P. Tosi, and G. Vignale, *Phys. Rev. B* **71**, 045323 (2005).
- ²⁹ M. Polini, R. Asgari, Y. Barlas, T. Pereg-Barnea, and A.H. MacDonald, *Solid State Commun.* **143**, 58 (2007); M. Polini, R. Asgari, G. Borghi, Y. Barlas, T. Pereg-Barnea, and A.H. MacDonald, *Phys. Rev. B* **77**, 081411(R) (2008).
- ³⁰ E.H. Hwang and S. Das Sarma, *Phys. Rev. B* **77**, 081412(R) (2008).
- ³¹ The Coulomb potentials $V_{\ell\ell'}(q)$ can be determined by solving the Poisson equation $\nabla^2\varphi(\boldsymbol{\rho}, z) = 0$ for the electrical potential $\varphi(\boldsymbol{\rho}, z)$ in cylindrical coordinates. The solution of the Poisson equation in all the $N + 1$ regions can be written as $\varphi_\ell(\boldsymbol{\rho}, z) = \exp(i\mathbf{q} \cdot \boldsymbol{\rho})[\alpha_\ell \exp(qz) + \beta_\ell \exp(-qz)]$ and depends on a total of $2(N + 1)$ constants. Two are fixed by imposing boundary conditions $\varphi(\boldsymbol{\rho}, z \rightarrow \pm\infty) = 0$ at infinity. The remaining $2N$ constants are fixed by the continuity of the potential φ across each layer and by imposing that the electric displacement has a discontinuity. Let $D_\ell = \epsilon_\ell E_\ell$ be the electric displacement above the ℓ -th layer and ϵ_ℓ be the dielectric constant in this region of space ($E = -\partial_z\varphi$). Then one has to impose that $D_{\ell+1} - D_\ell = 4\pi\sigma_\ell$ for $\ell = N \dots 1$, where $\sigma_\ell = -e$ is the Fourier transform of $-e\delta^2(\boldsymbol{\rho})\delta(z - (\ell - 1)d)$.
- ³² L. Zheng and A.H. MacDonald, *Phys. Rev. B* **49**, 5522 (1994).
- ³³ J. Gonzáles, F. Guinea, and M.A.H. Vozmediano, *Phys. Rev. B* **59**, 2474(R) (1999); E.G. Mishchenko, *Phys. Rev. Lett.* **98**, 216801 (2007); S. Das Sarma, E.H. Hwang, and W.-K. Tse, *Phys. Rev. B* **75**, 121406(R) (2007); D.E. Sheehy and J. Schmalian, *Phys. Rev. Lett.* **99**, 226803 (2007).
- ³⁴ M. Polini, A. Tomadin, R. Asgari, and A.H. MacDonald, *Phys. Rev. B* **78**, 115426 (2008).